

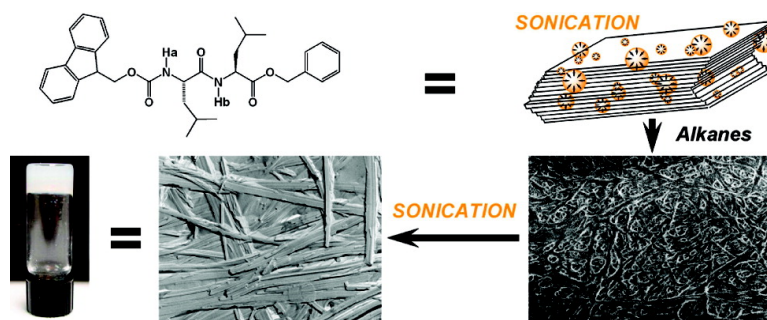
Communication

**Unusual Sculpting of Dipeptide Particles by Ultrasound Induces Gelation**

David Bardelang, Franck Camerel, James C. Margeson, Donald M. Leek, Marc Schmutz, Md. Badruz Zaman, Kui Yu, Dmitriy V. Soldatov, Raymond Ziessel, Christopher I. Ratcliffe, and John A. Ripmeester

*J. Am. Chem. Soc.*, **2008**, 130 (11), 3313-3315 • DOI: 10.1021/ja711342y

Downloaded from <http://pubs.acs.org> on February 8, 2009



**More About This Article**

Additional resources and features associated with this article are available within the HTML version:

- Supporting Information
- Links to the 5 articles that cite this article, as of the time of this article download
- Access to high resolution figures
- Links to articles and content related to this article
- Copyright permission to reproduce figures and/or text from this article

[View the Full Text HTML](#)

## Unusual Sculpting of Dipeptide Particles by Ultrasound Induces Gelation

David Bardelang,<sup>\*,†</sup> Franck Camerel,<sup>\*,‡</sup> James C. Margeson,<sup>§</sup> Donald M. Leek,<sup>†</sup> Marc Schmutz,<sup>||</sup> Md. Badruz Zaman,<sup>†</sup> Kui Yu,<sup>†</sup> Dmitriy V. Soldatov,<sup>⊥</sup> Raymond Ziessel,<sup>‡</sup> Christopher I. Ratcliffe,<sup>\*,†</sup> and John A. Ripmeester<sup>†</sup>

Steeacie Institute for Molecular Sciences, National Research Council of Canada, 100 Sussex Drive, Ottawa, Ontario K1A0R6 Canada, Laboratoire de Chimie Moléculaire, ECPM, UMR 7509, CNRS – Université Louis Pasteur, 25 rue Becquerel, 67087 Strasbourg Cedex 02 France, Institute for Research in Construction, National Research Council of Canada, 1200 Montreal Road, Ottawa, Ontario K1A0R6, Canada, Institut Charles Sadron, CNRS – UPR 22, 6 rue Boussingault, 67083 Strasbourg France, and Department of Chemistry, University of Guelph, 50 Stone Road, East, Guelph, Ontario N1G2W1 Canada

Received December 21, 2007; E-mail: christopher.ratcliffe@nrc-cnrc.gc.ca

Recently, ultrasound has emerged to play unexpected roles in physics and chemistry, for example causing mechano-<sup>1</sup> and sonoluminescence,<sup>2</sup> or to bias classical reaction pathways to reach unexpected products.<sup>3,4</sup> Another intriguing example of this peculiar influence of ultrasound was first described by Naota and co-workers regarding organogelation by pallado-macrocycles.<sup>5</sup> This result was extended recently to new peptide-based palladium complexes.<sup>6</sup> In these two cases, the mechanism involved conformational changes of the gelator triggered by a period of sonication which induces supramolecular self-assembly leading to gelation of the liquid. Such an unusual way to induce gelation is highly interesting, as it seems counterintuitive that application of ultrasound will be compatible with the successive self-assembly events leading to a gelation with a low molecular weight gelator through the formation of weak intermolecular interactions.<sup>7,8</sup> Indeed, ultrasound is usually used in laboratories and in food industries to disrupt weak intermolecular interactions, to solubilize molecules, or to disperse particles. Here we describe the basis of a new gelation mechanism based on a readily prepared dipeptide, in which ultrasound modifies the morphology of the material from sheet-like particles into 3-dimensional networks of fibers or ribbons, which are responsible for gelation.

Dipeptide **1** was prepared in a single step procedure from *N*-Fmoc-protected Leucine and *C*-benzoyl-protected Leucine by peptidic coupling in acetonitrile (Figure 1 and ESI for synthesis). Although dipeptide **1** was soluble in a wide variety of solvents at 20 °C, it was soluble in water and cyclic and linear alkanes (Table S1, Supporting Information) only at elevated temperatures. The cooling of hot (~80 °C) homogeneous alkane solutions of compound **1** did not result in gel formation and the compound precipitated out of the solutions (systematic precipitation for hexane in the 25–100 mM concentration range). However, when dispersions of dipeptide **1** in alkanes (*c* = 26 mM) were submitted to sonication at 20 °C for a period of 1–4 min(s), a complete and homogeneous liquid gelation was observed (Figure 1). Gelation was only observed when ultrasound was used as an external stimulus. The temperature of the sonication bath was found to be crucial since high temperatures prevent gel formation (*T* > 45 °C). The critical gelation concentration was found to be around 10 mM in hexane. The gels are white, opaque, and stable for months at room temperature. Interestingly, mixtures of polar solvents could also be gelled by compound **1** as for example in water/methanol. This

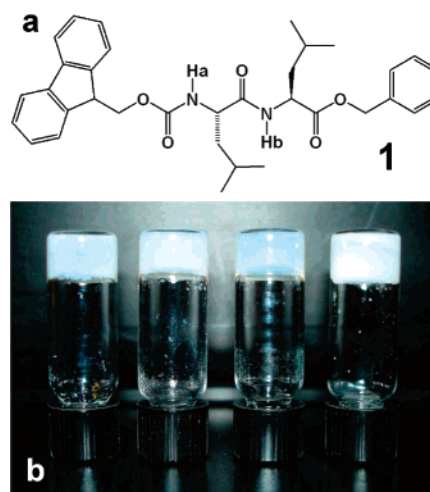


**Figure 1.** (a) Molecular structure of dipeptide **1**; (b) gels formed after submitting **1** to sonication (40.0 kHz, 0.28 W·cm<sup>-2</sup>) in various alkanes or a mixture of polar solvents at 20 °C (*c* = 26 mM) (from left to right: *n*-hexane, *n*-hexadecane, cyclohexane, and water/methanol (20/80 vol %) (*t*<sub>sonic</sub> = 60 s, except for *n*-hexadecane *t*<sub>sonic</sub> = 240 s).

seems to be a unique feature of the present dipeptide since molecules lacking the benzoyl group or with a benzoyl replacing the Fmoc group do not show any solvent gelation by ultrasound.

Scanning electron microscopy (SEM) was used to investigate the mechanism of gel formation in hexane. The as-synthesized material is composed of nano- to micrometer size sheet-like particles (Figure 2a). Dipeptide **1** immersed in hexane for several days prior to solvent evaporation and imaging remains essentially identical in appearance to the as-prepared material (see Figure S2, Supporting Information). Likewise, when the dipeptide is dispersed in hexane followed by a heating–cooling cycle, well-defined sheets are clearly visible from the precipitate (Figure 2b). On the other hand, dramatic morphological changes are observed from samples subjected to ultrasound. After only 10 s of sonication (Figure 2c), the micrographs clearly indicate a restructuring of the sheet via the appearance of tiny holes and wrinkling of the surface. Longer exposure to ultrasound (20 s, Figure 2d) confirms the emergence of holes. After 40 s exposure to ultrasound, SEM shows that the pore volume is dramatically expanded and the peptide particles have been reshaped from the *interior* (Figure 2e) revealing the appearance of an entangled network of fibers (Figure 2e, inset). After 60 s of sonication, the whole of the material was found to form a well defined extended network of thinner fibers (Figure 2f) in accord with the visual observation of a gel state. In a water/methanol

<sup>†</sup> Steacie Institute for Molecular Sciences.

<sup>‡</sup> Université Louis Pasteur.

<sup>§</sup> Institute for Research in Construction.

<sup>||</sup> Institut Charles Sadron.

<sup>⊥</sup> University of Guelph.

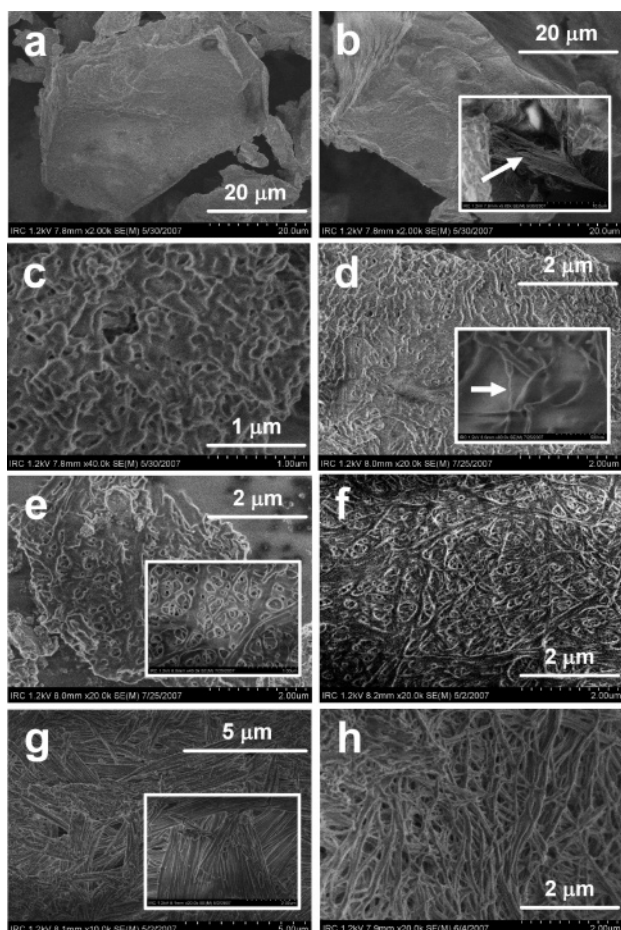


**Figure 2.** SEM micrographs obtained: (a) on the as-synthesized dipeptide; (b) on the precipitate isolated after a heating and cooling cycle in hexane; (c) after 10 s sonication in hexane; (d) after 20 s sonication in hexane; (e) after 40 s sonication in hexane; (f) after 60 s sonication in hexane; (g) after 10 min sonication in hexane; (h) after 60 s sonication in a water/methanol mixture (20/80 vol %). All images were recorded from xerogels and dried solutions/suspensions prepared using 5 mg of dipeptide **1** dispersed into 350  $\mu\text{L}$  of solvent.

mixture (20/80 vol %), the formation of well-defined fibers with an average diameter of 60 nm is also clearly observed after 60 s of sonication (Figure 2h).

Longer exposure of the dipeptide dispersion to ultrasound (10 min) resulted in the formation of straight ribbon-like objects (Figure 2g). The formation of ribbon-like structures for longer sonication times was also confirmed by freeze fracture electron microscopy experiments performed on a nonane gel ( $c = 26$  mM, 90 s ultrasound). Well-defined ribbons, with a width ranging from 20 to 100 nm, with an average of  $\sim 50$  nm, and a length up to several micrometers are clearly visible (Figure 3). This is in excellent agreement with observations by SEM of samples sonicated for longer than 1 min. The ribbon structures likely represent the final architecture after the ultrasound has reshaped the peptide particles with the formation of fiber networks as an intermediate structure.

To gather information at the molecular level, liquid state  $^1\text{H}$  NMR experiments were performed. A 2D-NOESY spectrum of a  $\text{CDCl}_3$  solution of dipeptide **1** at 295 K revealed the existence of several conformations, whereas a unique conformation was deduced from the NMR spectra ( $^1\text{H}$ ,  $^1\text{H}-^1\text{H}$  COSY, and 2D-ROESY) of a  $d_{1,4}$ -hexane solution ( $c = 15$  mM) at 60  $^\circ\text{C}$ . ROE cross-peaks are in line with an *anti* conformation presenting the two amide functions (and also isobutyl chains) in opposite directions (Figure S3, Supporting Information).

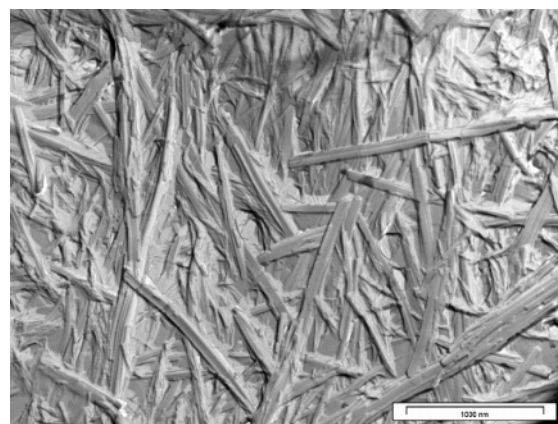


**Figure 3.** Freeze fracture electron micrograph obtained with a nonane gel prepared with dipeptide **1** at 26 mM concentration after a sonication time of 90 s.

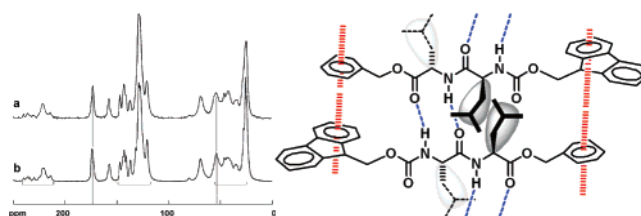


**Figure 4.** (left) Solid-state CP-MAS  $^{13}\text{C}$  NMR spectra of (a) the precipitate (spin rate = 7 kHz), (b) the xerogel (7 kHz). (Right) Proposed antiparallel  $\beta$ -sheet model for compound **1** in the as-synthesized material and in the gel.

Such a conformation is favorable for the organization of the dipeptide inside  $\beta$ -sheet structures via intermolecular hydrogen bonding, a structure often encountered in natural and synthetic oligopeptides (Figure 4).<sup>9</sup>

Solid-state cross-polarization magic angle spinning (CP-MAS)  $^{13}\text{C}$  NMR spectra of as-synthesized material, a xerogel (desolvated gel) obtained after slow evaporation of the solvent, and a gel with nonane exhibit essentially the same patterns (Figure 4, left-hand-side and Figure S5, Supporting Information). All three materials show carbonyl and  $\text{C}\alpha$  peaks at  $\sim 173$  and 53 ppm respectively, characteristic of sheet rather than helical structures for which the resonances are expected at  $\sim 179$  and 58 ppm, respectively.<sup>10</sup> These results indicate a similar molecular organization in the as-synthesized material and in the gel, a result confirmed by FT-IR spectroscopy. A unique NH band centered at  $3302\text{ cm}^{-1}$  is observed and is typical of NH functions engaged in hydrogen bonding. Free NH functions are found at  $3430\text{ cm}^{-1}$  in chloroform. In  $\text{CHCl}_3$  solution, three stretching  $\nu_{\text{C}=\text{O}}$  bands at  $1732$ ,  $1716$ , and  $1679\text{ cm}^{-1}$  are attributed to unbound ester, carbamate, and amide carbonyl functions, respectively. In the solid, gels, and xerogels, all the amide functions are engaged in hydrogen bonding ( $\nu_{\text{C}=\text{O}} 1648\text{ cm}^{-1}$ ), whereas the carbonyl band of the carbamate function is split into two equal bands at  $1716$  and  $1693\text{ cm}^{-1}$ . Regarding the results obtained in  $\text{CHCl}_3$ , the first  $\nu_{\text{C}=\text{O}}$  stretching vibration is characteristic of free carbamate and the second to hydrogen-bonded carbamate. These observations are in line with the proposed model where half of the carbamate functions are hydrogen bonded. Thus, the overall set of data suggests the formation of  $\beta$ -sheet-like structures via intermolecular hydrogen bonding in which an *anti* conformation is favored. The gelation seems to rely on a morphological change of the dipeptide particles induced by a sonocrystallization process rather than changes in the aggregation mode or in the conformation of the molecule inside the material.



**Figure 5.** Selective organic liquid gelation over water (1/1 vol %). From left to right: paraffin oil, olive oil, and kerosene ( $[1] = 26 \text{ mM}$ ,  $700 \mu\text{L}$ ) after 2 min sonication. The aqueous phase (top) is trapped by the gel.

To gain better insights into the evolution of the morphology of the material, X-ray diffraction and differential scanning calorimetry (DSC) experiments have been performed on the as-synthesized material and on xerogels (Figure S6, Supporting Information).

From X-ray experiments, it can be seen clearly that the material is more crystalline in the xerogel than in the as-synthesized material. In fact, sharp reflections are observed in the  $5\text{--}35^\circ 2\theta$  range for the xerogels whereas only a very broad feature centered at  $2\theta = 20^\circ$  was observed in the starting material. The crystallization of the material upon sonication was also confirmed by DSC as the traces reveal that upon sonication the material becomes more structured and the endothermic peak at  $93^\circ\text{C}$  (due to melting) for the starting material is gradually replaced by the sharper peak at  $102^\circ\text{C}$  corresponding to the xerogel obtained after 60 s sonication. These results indicate that a crystallization of the material upon sonication is at the origin of the gelation (sonocrystallization).<sup>11</sup> This process also accounts for the formation of the stiff ribbons observed by SEM and FFEM for longer sonication times. It should be noted that the precipitate obtained after heating/cooling cycles, and that particles exposed to solvents for several days but without application of ultrasound, remains poorly organized. A dissolution-reassembly due to the high local temperature and pressure generated by the ultrasound may be at the origin of this sonocrystallization process.<sup>4,8,11</sup>

The insolubility of the dipeptide in alkanes and water at  $20^\circ\text{C}$  prompted us to see whether selective gelation of water/organic liquid mixtures could be induced with the aid of ultrasound. Effectively, when two equal volumes of the organic phase and water are mixed together followed by exposure to ultrasound for 2 min, a milky emulsion formed. Separation of the liquids then took place at different times depending on the particular water/cosolvent mixture and in each case it was the organic liquid (paraffin oil, olive oil, kerosene) which gelled (Figure 5).

Therefore, this unique dipeptide/ultrasound process is able to selectively gel oil in water without heat and may well open new avenues for real-life applications such as the decontamination of oil spills.<sup>12</sup>

In conclusion, ultrasound has been used advantageously to reshape sheet-like dipeptide particles into elongated molecular assemblies which are at the origin of solvent gelation. A sonocrystallization process appears to be at the main origin of the gelation. Sonication time, temperature, and solvents were found to play a crucial role in determining the morphology of the particles, features which are particularly appealing for templating materials.<sup>13</sup> This is a clear and rare example of how dipeptides can display remarkable behavior when subjected to ultrasound.

**Acknowledgment.** The National Research Council Canada is acknowledged for financial support. We are also grateful to Dr. Stephen Lang and Malgosia Daroszewska for technical assistance.

**Supporting Information Available:** Preparation and full characterization of dipeptide **1**, a table of solvents tested for gelation, additional photographs, SEM, a ROESY NMR spectrum, solid state NMR spectra, differential scanning calorimetry, and powder X-ray diffraction measurements. This material is available free of charge via the Internet at <http://pubs.acs.org>.

## References

- (1) Eddingsaas, N. C.; Suslick, K. S. *Nature* **2006**, *444*, 163.
- (2) (a) Suslick, K. S.; Flint, E. B. *Nature* **1987**, *330*, 553–555. (b) Didenko, Y.; McNamara, W. B., III.; Suslick, K. S. *Nature* **2000**, *407*, 877–879. (c) Flannigan, D. J.; Hopkins, S. D.; Camara, C. G.; Putterman, S. J.; Suslick, K. S. *Phys. Rev. Lett.* **2006**, *96*, 204301-1–4.
- (3) Hickenboth, C. R.; Moore, J. S.; White, S. R.; Sottos, N. R.; Baudry, J.; Wilson, S. R. *Nature* **2007**, *446*, 423–427.
- (4) Cravotto, G.; Cintas, P. *Angew. Chem., Int. Ed.* **2007**, *46*, 5476–5478.
- (5) Naota, T.; Koori, H. *J. Am. Chem. Soc.* **2005**, *127*, 9324–9325.
- (6) Isozaki, K.; Takaya, H.; Naota, T. *Angew. Chem., Int. Ed.* **2007**, *46*, 2855–2857.
- (7) Baddeley, C.; Yan, Z.; King, G.; Woodward, P. M.; Badji, J. D. *J. Org. Chem.* **2007**, *72*, 7270–7278.
- (8) Paulusse, J. M. J.; van Beek, D. J. M.; Sijbesma, R. P. *J. Am. Chem. Soc.* **2007**, *129*, 2392–2397.
- (9) (a) Tycko, R. *Quat. Rev. Biophys.* **2006**, *39*, 1–55. (b) Tycko, R. *Curr. Op. Struct. Bio.* **2004**, *14*, 96–103.
- (10) (a) Baxa, U.; Wickner, R. B.; Steven, A. C.; Anderson, D. E.; Marekov, L. N.; Yau, W.-M.; Tycko, R. *Biochemistry* **2007**, *46*, 13149–13162. (b) Lim, K. H.; Nguyen, T. N.; Damo, S. M.; Mazur, T.; Ball, H. L.; Prusiner, S. B.; Pines, A.; Wemmer, D. E. *Solid State NMR* **2006**, *29*, 183–190.
- (11) Ruecroft, G.; Hipkiss, D.; Ly, T.; Maxted, N.; Cains, P. W. *Org. Process Res. Dev.* **2005**, *9*, 923–932 and references therein.
- (12) (a) Bhattacharya, S.; Krishnan-Ghosh, Y. *Chem. Commun.* **2001**, 185–186. (b) Trivedi, D. R.; Dastidar, P. *Chem. Mater.* **2006**, *18*, 1470–1478.
- (13) (a) van Bommel, K. J. C.; Friggeri, A.; Shinkai, S. *Angew. Chem., Int. Ed.* **2003**, *42*, 980–999 and references therein. (b) Roy, G.; Miravet, J. F.; Escuder, B.; Sanchez, C.; Llusar, C. *J. Mater. Chem.* **2006**, *16*, 1817–1824. (c) Ray, S.; Das, A. K.; Banerjee, A. *Chem. Commun.* **2006**, 2816–2818. (d) Bhattacharya, S.; Srivastava, A.; Pal, A. *Angew. Chem., Int. Ed.* **2006**, *45*, 2934–2937.

JA711342Y